Polymer(Korea), Vol. 41, No. 5, pp. 820-826 (2017)
https://doi.org/10.7317/pk.2017.41.5.820

ISSN 0379-153X(Print)
ISSN 2234-8077(Online)

마이크로파 박리공정에 의한 비작용기화 그래핀 및 폴리프로필렌 카보네이트 기반의 나노 복합물질

오혁균 · 김성우†
경기대학교 화학공학과
(2017년 3월 10일 접수, 2017년 4월 19일 수정, 2017년 4월 19일 채택)

Poly(propylene carbonate) Nanocomposites Incorporating Non-functionalized Graphene Nanosheets Prepared by Microwave-assisted Exfoliation Process

Hyeok Gyun Oh and Seong Woo Kim†
Department of Chemical Engineering, Kyonggi University, 154-42 Gwanggyosan-ro, Yeongton-gu, Suwon 16227, Korea
(Received March 10, 2017; Revised April 19, 2017; Accepted April 19, 2017)

초록: 비작용기화 그래핀 나노 판상체(non-functionalized graphene nanosheets, NFGNs)와 생분해성 폴리프로필렌 카보네이트(PPC) 수지를 용액 블렌딩 공정을 이용하여 혼합함으로써 제반 물성 및 차단 특성이 향상된 나노 복합필름을 제조하였다. 그래파이트에 마이크로파를 조사하여 팽창시킨 이후 연속적으로 초음파 분산공정을 이용하여 층간 간격이 증가된 삽입 및 박리 구조를 갖는 NFGNs를 얻었다. 다양한 함량의 NFGNs를 함유한 나노 복합필름의 유리전이온도, 인장 물성 및 산소투과율을 측정하였으며, 이로부터 NFGNs 첨가가 PPC 수지의 열적, 기계적 성질 및 가스 차단 성능의 향상에 미치는 영향을 조사하였다. NFGNs를 1.0 wt% 이하의 적은 함량으로 첨가하여도 열적, 기계적 성질 및 차단 특성이 매우 뚜렷하게 향상된 것으로 나타났다. NFGNs를 혼합한 나노 복합필름의 투명성은 광 산란의 증가로 인하여 순수 PPC 필름에 비해 감소하였으나, 0.3 wt% 함량으로 혼합한 경우에는 광투과율 80% 정도의 비교적 우수한 투명성을 나타냈다.

Abstract: Biodegradable poly(propylene carbonate) (PPC)-based nanocomposite films with enhanced physical and barrier properties were prepared by incorporating non-functionalized graphene nanosheets (NFGNs) via solution blending. The highly intercalated and exfoliated NFGNs were successfully obtained by employing microwave irradiation-assisted exfoliation method, followed by sonication. The thermal and mechanical reinforcement and gas barrier effects arising from incorporation of NFGNs into PPC were investigated in terms of measurements of glass transition temperature, tensile properties, and oxygen transmission rate for the resultant nanocomposite films with various loadings. The remarkable improvement in the thermal, mechanical, and barrier properties was achieved by the incorporation of only small amounts of NFGNs below 1.0 wt%. The incorporation of NFGNs decreased the optical transparency of the film because of increased light scattering, but 0.3 wt% NFGNs loading gave rise to fairly good transparency with a light transmission of around 80%.

Keywords: poly(propylene carbonate), non-functionalized graphene nanosheets, microwave irradiation, nanocomposite film.

Introduction

Aliphatic poly(propylene carbonate) (PPC) synthesized from carbon dioxide and propylene oxide has drawn much attention in both research and industry owing to its eco-friendly nature leading to reduction of the amount of carbon dioxide as well as biodegradability.[1,2] Moreover, a completely amorphous PPC resin has potentially wide range of applications for packaging materials because of its excellent ductility, good melt flow characteristics, and high barrier property.[3]

In spite of such advantages of biodegradable PPC resin, it still shows a limitation in the practical application of packaging films due to its inferior thermal and mechanical properties relative to traditional undegradable polymers. Accordingly, much

†To whom correspondence should be addressed.
E-mail: wookim@kyonggi.ac.kr

efforts have recently been dedicated to improving the properties of PPC by incorporating nanofillers such as organically modified nanoclay platelets and organic cellulose nanofibers (CNFs), or blending it with other polymers.[3-6] A fairly large amount of nanoclay platelets and CNFs (~10 wt%) with nanoscale dimensions has been incorporated into polymer matrices to achieve the substantial reinforcing effect caused by nanofiller loading. Furthermore, such nanofiller-based nanocomposites showed a limitation in improvement of physical performances because of the relatively low surface area of the incorporated nanoclay platelets and CNFs with restricted aspect ratios.

Graphene, a monolayer of carbon atoms arranged in a two-dimensional honeycomb structure, has recently attracted great attention in the field of nanofiller-based polymer nanocomposites owing to its exceptional performances such as mechanical, thermal, electrical, and gas barrier properties. In particular, graphene, as a nanofiller with atomically thin structure, is a promising alternative to nanoclay platelets, carbon nanotubes (CNT) and CNFs. It could effectively improve the physical and barrier properties of nanocomposites even with very low level of loading, because of its extremely high specific surface area, large aspect ratio, and tightly packed planar structure.[7-10] Among the various graphenes, chemically functionalized or modified graphene oxide nanosheets with oxygen-containing functional groups have mainly been used to produce the polymer nanocomposites, because the bulky functional groups formed on their surfaces can promote the intercalation of graphite stacked layers followed by exfoliation during the mixing process, resulting in homogeneous dispersion of highly exfoliated graphene nanosheets in polymer matrix.[11-19] In preparing graphene oxide, however, severe oxidation and introduction of a number of functional groups may induce the significant lateral size reduction from the parent graphite as well as generation of defects on its surface.[7,14] Moreover, the manufacturing of exfoliated graphene oxide solution is economically infeasible, because it involves many processing steps such as preoxidation, mixing, oxidation, and solvent exchange. As an alternative to functionalized graphene oxide nanosheets (GONs), non-functionalized graphene nanosheets (NFGNs), such as exfoliated graphene (EG)[21-23] and thermally or chemically reduced graphene,[24,25] have also been used to prepare graphene-based polymer nanocomposites with improved properties. Several methods for preparing EG or exfoliated graphene oxide (EGO) have been reported. These include subjecting the pristine graphite to the heating source, coupled plasma, laser irradiation and microwave (MW) irradiation.[26,27] Of these, MW irradiation is recognized as very efficient method because of its relatively low processing temperature, short processing time and less consuming energy.[28]

In this study, the simple exfoliation method by microwave irradiation as a rapid and efficient route was employed to prepare non-functionalized graphene nanosheets (NFGNs). We prepared biodegradable PPC-based nanocomposite films with improved performances by incorporating the NFGNs as reinforcement as well as gas barrier via solution blending method. We investigated the effects of the level of NFGNs loading on the morphology, thermal, mechanical, optical, and gas barrier properties of the prepared PPC/NFGNs nanocomposite films in terms of SEM observation, glass transition temperature, tensile strength/modulus, visible light transmittance, and oxygen transmission rate (OTR). We also demonstrated the feasibility of applying the NFGNs by simple microwave-assisted exfoliation process to the production of high performance nanocomposites.

Experimental

Materials. Poly(propylene carbonate) resin (PPC, GreenPol™, SK Innovation Co.) with weight-average molecular weight of 185360 g/mol was used as an organic polymer matrix in the graphene/PPC nanocomposites. Natural graphite powders purchased from Sigma-Aldrich have an average particle size of 140 μm. Potassium permanganate ($KMnO_4$, 99%, Sigma-Aldrich) and nitric acid (HNO_3, 65%, Duksan) were used as the oxidant and intercalation agent for oxidizing the partial edge area of natural graphite under MW irradiation. *N*,*N*-dimethylformamide (DMF, Duksan) for dissolution of the PPC and dispersion of the graphene nanofillers was used throughout the experiments. The materials were used as received without further purification.

NFGNs were prepared from natural graphites via microwave-assisted intercalation and exfoliation process followed by sonication. The natural graphites (0.5 g), $KMnO_4$ (1.0 g) and HNO_3 (0.34 mL) were only simply mixed in a crucible before MW irradiation, and the mixture was placed in an electronic microwave oven (MWO20MC1, Tongyang magic Inc., 700 W) to cause intercalation and exfoliation of the graphites under MW irradiation for 40 s. Figure 1 shows the digital images of the pristine graphite and the expanded graphite powders prepared from MW irradiation, respectively. As compared with pristine graphite, the remarkable increase in volume of the

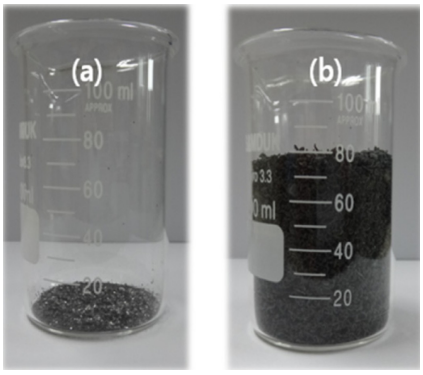

Figure 1. Digital micrographic images of (a) pristine graphite; (b) expanded graphite after MW irradiation.

graphite powders is caused by MW irradiation. The resultant expanded graphite powders were then dispersed in DMF solvent via vigorous sonication for 30 min using ultrasonicator (VCX500, Sonics & Materials Inc.) to obtain a NFGNs solution with a highly exfoliated structure of the dispersed nanofiller.

Preparation of Nanocomposite Films. The PPC/NFGNs nanocomposite thin films with a thickness of ca. 40 μm were prepared via solution-processed blending and casting method. PPC resin in pellet form was dissolved in DMF by magnetic stirring at room temperature to prepare a homogeneous PPC solution. A specific amount of NFGNs suspension in DMF was then added to the PPC solution under vigorous sonication for 10 min, followed by magnetic stirring for 48 h. The resulting PPC/NFGNs solution with a homogeneous dispersion was deposited on a glass substrate, and then casted using a micrometer film applicator (REF 1117, SI Co.). The casted films were dried at 60 ºC in a drying oven for 2 h. The dried PPC/NFGNs thin film was cautiously detached from the glass substrate. The content of incorporated NFGNs in the nanocomposite samples was set at 0.3, 0.6, and 1.0 wt%. All the dried samples were kept in a dessicator to prevent the moisture influence prior to performing characterization.

Characterization. An X-ray diffractometer (XRD, D/MAX-2500, Rigaku Co.) was used to quantitatively analyze the intercalated or exfoliated nanostructure of NFGNs as prepared and the NFGNs as dispersed in the PPC matrix. The Cu Kα radiation source was operated at 40 kV and 150 mA. The scanning rate was 1.0º/min in the range of 5-40º. The nanostructured-morphologies of the nanofillers and PPC/NFGNs nanocomposites were observed by using a scanning electron microscope (SEM, S-4800, Hitachi Co.). The pristine graphite, expanded graphite, and NFGNs were in the form of powder, whereas the PPC/NFGNs nanocomposite samples were from fracture surface films. Differential scanning calorimetry (DSC1, Mettler Toledo Co.) was used to examine the thermal properties such as glass transition temperature (T_g) for the nanocomposites with various NFGNs loadings. The samples were initially heated from room temperature to 80 ºC, then cooled to -20 ºC at a rate of 20 ºC/min, and finally heated again to 80 ºC at a heating rate of 10 ºC/min under nitrogen gas flow. The thermal properties were analyzed based on the second heating thermograms. The optical transparency in the visible-light wavelength range of 550 - 850 nm for the prepared PPC/NFGNs nanocomposite film was evaluated by using a visible spectrophotometer (Optizen 2120UV, Mecasys Co., Korea). The tensile properties of the nanocomposite films were measured using a universal testing machine (QM100S, Qmesys Co.) operating at 30 mm/min of cross-head speed. Five samples with dimensions of 15 mm (width)×50 mm (length) were tested and an average value was determined from the data. The oxygen transmission rate (OTR) through the nanocomposite film was measured at 23 ºC and 0% relative humidity using an oxygen permeability tester (OX-TRAN 2/10, MOCON Inc.).

Results and Discussion

The nanostructures of pristine graphite, intermediate expanded graphite and exfoliated NFGNs were qualitatively examined by SEM observation. The SEM images of such nanofillers in Figure 2 demonstrate that the original pristine graphite flake has a microstructure of very closely stacked graphitic layers. Upon MW irradiation, the graphite precursor is expanded and markedly separated into individual graphene nanosheets with a crumpled appearance. The porous medium-like structure with connections between layers can be clearly seen in Figure 2(b). The subsequent physical treatment of sonication after MW irradiation can cause further separation and breakage of linked graphitic layers, finally resulting in NFGNs with highly exfoliated nanostructure as shown in Figure 2(c). From the micrographs, the thickness and width of the NFGNs were approximately estimated to be 5.6~10.5 nm and 3.5~6.5 μm, respectively. The microstructures of the nanofillers and nanocomposite were also evaluated by XRD analysis as quantitative method. Figure 3 shows the XRD patterns in the 2θ range of 5-40º for the various samples. The characteristic sharp diffraction peak at 2θ=26.4º for the pristine natural graphite corresponds to an interlayer spacing (d_{002}) of 0.34 nm between the graphitic layers. In the case of NFGNs sample, however,

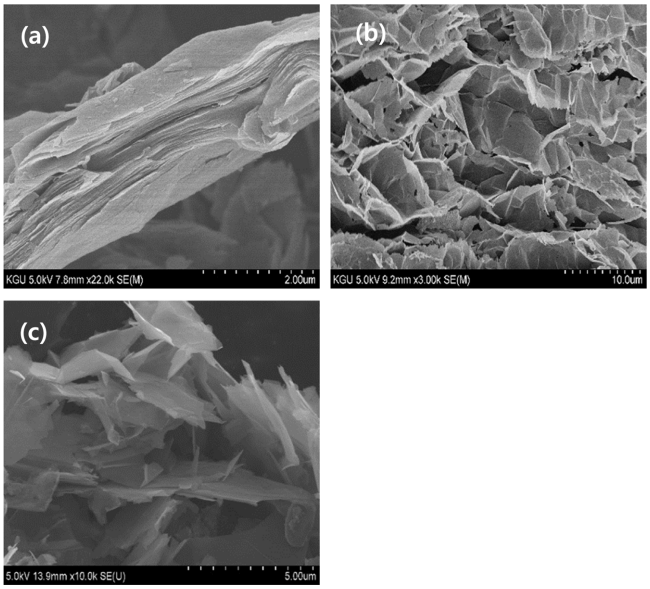

Figure 2. SEM images of (a) pristine graphite; (b) expanded graphite; (c) NFGNs.

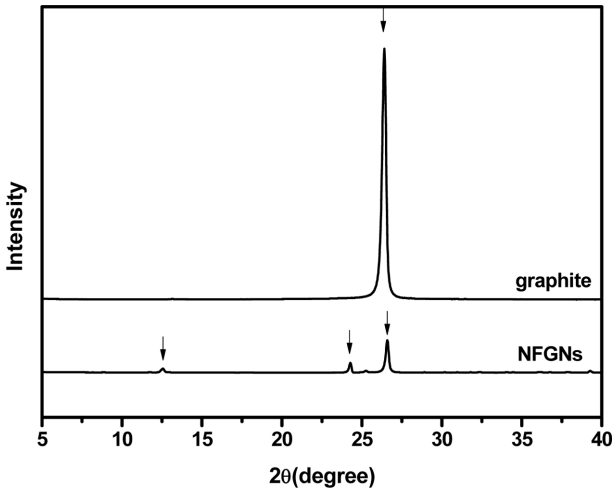

Figure 3. XRD patterns of pristine graphite and NFGNs.

this characteristic peak diminished considerably, and another two very weak peaks at different 2θ locations were observed, indicating that most of the graphites were completely exfoliated, but some of few graphene layers maintained the status of the original stacked graphite, and there were two intercalated graphene tactoids with interlayer distance of 0.37 nm (2θ=24.3°) and 0.70 nm (2θ=12.6°). The morphologies of the prepared PPC/NFGNs nanocomposites were also observed by SEM in order to examine the dispersion state of NFGNs in the PPC matrix and the structural variations of the nanofiller itself after solution blending. Figure 4 shows the SEM images of the

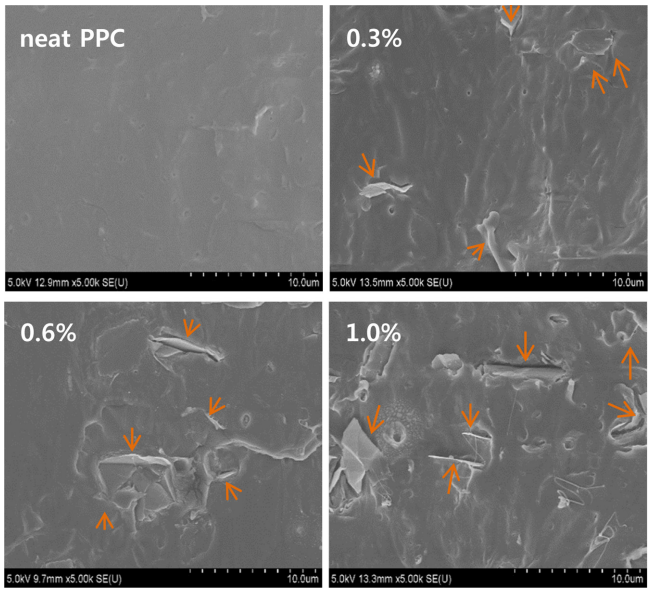

Figure 4. SEM images of neat PPC and corresponding nanocomposites with various NFGNs loadings.

fractured surfaces of neat PPC and nanocomposite films with various NFGNs loadings. The neat PPC displays a fairly even and smooth surface without any traces of nanofiller inclusion. For the nanocomposites with 0.3-1.0 wt% NFGNs, on the other hand, the exfoliated individual NFGNs and stacked thin tactoids with only a few layers were observed to be randomly dispersed in the PPC matrix. In addition, some agglomerated thick tactoids with larger domain can also be detected in the 1.0 wt% NFGNs loaded nanocomposite, suggesting that restacking occurred during solution blending, which may be due to cumulative strong van-der Waals interaction between graphitic layers without functional groups on their surfaces.[29]

In the nanocomposite based on completely amorphous polymers such as PPC, the glass transition temperature (T_g) has been recognized to be significant parameter for evaluating thermal performance of the final nanocomposite. The thermal reinforcing effect caused by incorporation of NFGNs into PPC resin was examined in terms of measurement of glass transition temperature of the nanocomposites. It has been known that the glass transition temperature of hydrophilic polymer generally increases upon addition of nanofillers with functional groups on their surfaces, because of the restricted chain segmental mobility of the polymer in the nanocomposite, resulting from the strong interaction between functional groups contained in both polymer and nanofiller phases.[20,30] Such reinforcement of the thermal property has been reported for the hydrophilic polymer-based nanocomposites incorporated with

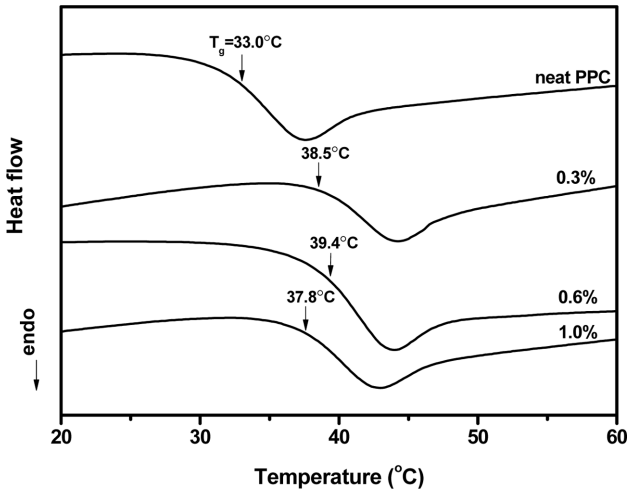

Figure 5. DSC heating thermograms of neat PPC and corresponding nanocomposites with various NFGNs loadings.

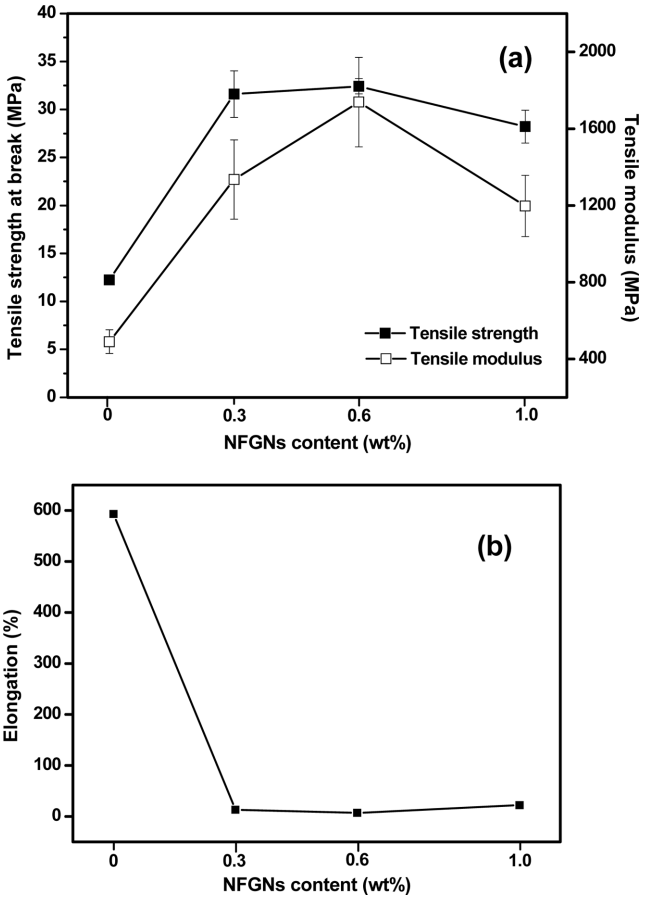

Figure 6. Mechanical properties of nanocomposite films with various NFGNs loadings: (a) tensile strength at break and tensile modulus; (b) elongation at break.

various functionalized nanofillers.[3,20,30,31] Figure 5 shows the DSC heating thermograms of neat PPC and corresponding nanocomposites with various NFGNs loadings. The incorporation of only small amount of NFGNs less than 1.0 wt% obviously increases the T_g value of the PPC resin in the nanocomposite, compared to that of neat PPC. When loaded with 0.6 wt% NFGNs, the nanocomposite exhibits the highest T_g at 39.4 °C, which is 6.4 °C higher than that of neat PPC. In the nanocomposites incorporated with NFGNs nanofillers utilized in this study, the remarkable increase in T_g value is also revealed, which may be due to interaction between hydrophobic segments in the PPC chain molecules and the hydrophobic surfaces of the non-functionalized graphene nanosheets.

The mechanical reinforcement arising from incorporation of graphene nanosheets with superior mechanical properties into PPC resin was also evaluated by performing tensile deformation test for the PPC/NFGNs nanocomposite films. Figure 6 shows the tensile properties of the nanocomposite films with various NFGNs loadings. As shown in the figure, the incorporation of NFGNs up to 0.6 wt% yields a dramatic increase in both tensile strength at break and modulus of the nanocomposite film by approximately 165% and 254%, relative to those of neat PPC film. Such a remarkable improvement in the tensile properties may originate from homogeneous dispersion of graphene nanosheets with a large aspect ratio and efficient stress transfer from the PPC matrix to the dispersed graphene nanofillers, which results from strong interaction between two phases as mentioned earlier. Further addition of NFGNs at 1.0 wt% decreases both tensile strength at break and modulus of the nanocomposite film, but still shows improved mechanical performance, compared with neat PPC film in our investigated range of NFGNs contents. On the other hand, elongation at break of the nanocomposite film is shown to be dramatically decreased from 593% of pure PPC to 13.1% and 6.8% by incorporation of NFGNs at 0.3 and 0.6 wt%, respectively. However, the nanocomposite film with 1.0 wt% loading shows increased elongation of 21.9%.

The flexible polymeric films for the application of packaging films generally require high optical transparency, which can allow the visual identification of materials inside the film. The deterioration in the optical transparency of the nanocomposite films can be expected because the nanofillers distributed within the film induce high degree of light scattering. Therefore, the effect of NFGNs incorporation on the optical transparency of the nanocomposite films prepared in this work was investigated to assess the possibility of application to packaging film. Figure 7 shows the relative visible light trans-

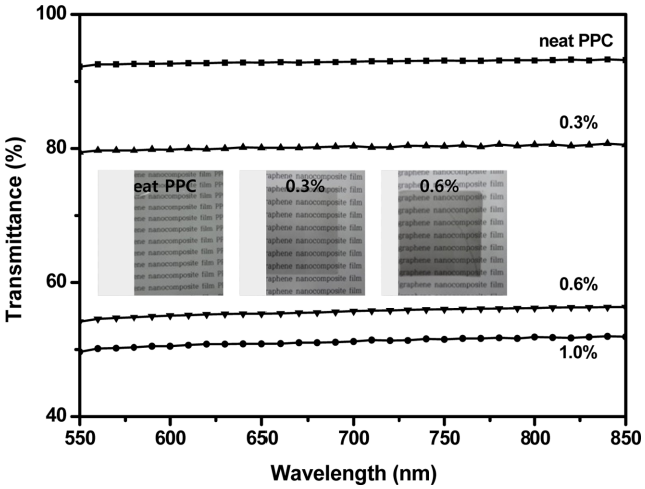

Figure 7. Visible light transmittance for the neat PPC film and corresponding nanocomposite films with various NFGNs loading.

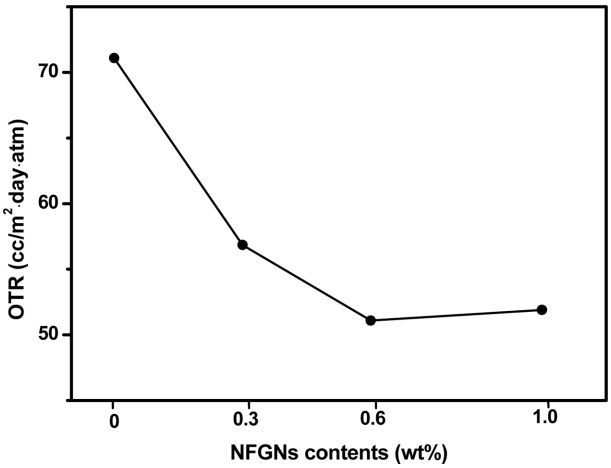

Figure 8. Oxygen transmission rate of NFGNs/PPC nanocomposite films with various NFGNs loadings.

mittance in the wavelength range of 550-850 nm for the neat PPC and its nanocomposite films with various NFGNs loadings. Owing to completely amorphous structure of PPC resin, the neat PPC film exhibits high optical transparency with light transmittance of around 93% in the whole wavelength range. When incorporated with NFGNs, the optical transparency of the nanocomposite film is reduced due to the increased light scattering and diffusivity through the film. The nanocomposite films with NFGNs loading over 0.6 wt% shows poor optical transparency with light transmittance below 60%, whereas 0.3 wt% NFGNs loaded film shows fairly good optical transparency with light transmittance of around 80%, presenting the possibility of utilization as packaging material.

The gas barrier performance is generally prerequisite for the application of nanocomposites to packaging films to preserve the quality of the products during storage.[32] The effect of NFGNs incorporation on the barrier properties of the nanocomposites was investigated by measuring the oxygen transmission rate (OTR) through the prepared nanocomposite films in the direction perpendicular to the film plane. Figure 8 shows the OTR for the neat PPC and its nanocomposite films with various NFGNs loadings from 0.3 to 1.0 wt%. The OTR of the nanocomposite films is reduced with increasing of NFGNs content up to 0.6 wt%, but it slightly increases at 1.0 wt% NFGNs loading. The dispersion of the planar-structured graphene nanosheet in the PPC matrix effectively increases the tortuous path for penetrating oxygen molecules, resulting in substantial decrease in OTR value. The oxygen barrier properties of the nanocomposite films containing only small amount of 0.3 and 0.6 wt% NFGNs are improved by 20% and 28.1%, respectively, relative to neat PPC film with an OTR of 71.1 cc m^{-2} day^{-1} atm^{-1}. However, the incorporation of NFGNs above 0.6 wt% does not contribute anymore to the improvement in the barrier property. It should be noted that the incorporation of NFGNs at 1.0 wt% content caused decrease in the thermal, mechanical, optical and barrier properties of the nanocomposites. Such a deterioration of all the properties of nanocomposite with 1.0 wt% loading may be attributed to poor graphene dispersion, which resulted from the occurrence of agglomerated thick tactoids with larger domain size, as observed in the SEM image of Figure 4.

Conclusions

The NFGNs at small loadings (0.3 to 1.0 wt%) were incorporated to produce biodegradable PPC-based nanocomposite films with reinforced physical performances as well as an improved gas barrier property. The NFGNs were prepared via a simple exfoliation process assisted by microwave irradiation, followed by sonication under solution state. XRD analysis and SEM observation showed that the NFGNs originally had a highly intercalated and exfoliated nanostructure, but some agglomerated graphitic tactoids were dispersed in the PPC matrix, because of re-stacking during solution blending and film casting. The incorporation of NFGNs at very small amounts up to 0.6 wt% into PPC resin could yield high performance nanocomposite films with substantially increased thermal property of T_g, tensile properties of strength at break and modulus, and improved oxygen barrier property. On the other hand, the nanocomposite film with excess loading of

NFGNs at 1.0 wt% showed slight deterioration in the physical and barrier properties, but it still retained improved performances, compared to neat PPC film.

Acknowledgement: This work was supported by Kyonggi University Research Grant 2015.

References

1. X. Hu, C. Xu, J. Gao, G. Yang, C. Geng, F. Chen, and Q. Fu, *Compos. Sci. Technol.*, **78**, 63 (2013).
2. X. Wang, Y. Xia, P. Wei, Y. Chen, Y. Wang, and Y. Wang, *J. Appl. Polym. Sci.*, **131**, 40832 (2014).
3. D. Wang, J. Yu, J. Zhang, J. He, and J. Zhang, *Compos. Sci. Technol*., **85**, 83 (2013).
4. X. Shi and Z. Gan, *Eur. Polym. J*., **43**, 4852 (2007).
5. C. Xing, H. Wang, Q. Hu, F. Xu, X. Cao, J. You, and Y. Li, *Carbohydr. Polym*., **92**, 1921 (2013).
6. M. Gao, Z. Ren, and S. Yan, *J. Phys. Chem. B*, **116**, 9832 (2012).
7. H. Kim, Y. Miura, and C. W. Macosko, *Chem. Mater*., **22**, 3441 (2010).
8. H.-D. Huang, P.-G. Ren, J. Chen, W.-Q. Zhang, X. Ji, and Z.-M. Li, *J. Memb. Sci*., **409**, 156 (2012).
9. L. Yu, Y. S. Lim, J. H. Han, K. Kim, J. Y. Kim, S. Y. Choi, and K. Shin, *Synth. Met*., **162**, 710 (2012).
10. H.-D. Huang, C.-Y. Liu, D. Li, Y.-H. Chen, G.-J. Zhong, and Z.-M. Li, *J. Mater. Chem. A*, **2**, 15853 (2014).
11. N. Yousefi, M. M. Gudarzi, Q. Zheng, X. Lin, X. Shen, J. Jia, F. Sharif, and J.-K. Kim, *Compos. Part A*, **49**, 42 (2013).
12. I.-H. Tseng, Y.-F. Liao, J.-C. Chiang, and M.-H. Tsai, *Mater. Chem. Phys*., **136**, 247 (2012).
13. S. W. Kim and H. M. Choi, *Korean J. Chem. Eng*., **33**, 330 (2016).
14. S. W. Kim and H. M. Choi, *High Perform. Polym*., **27**, 694 (2015).
15. S.-J. Lin, H.-J. Sun, T.-J. Peng, and L.-H. Jiang, *High Perform. Polym*., **26**, 790 (2014).
16. J. Wang, C. Xu, H. Hu, L. Wan, R. Chen, H. Zheng, F. Liu, M. Zhang, X. Shang, and X. Wang, *J. Nanopart. Res*., **13**, 869 (2011).
17. J. Bian, X. W. Wei, S. J. Gong, H. Zhang, and Z. P. Guan, *J. Appl. Polym. Sci*., **123**, 2743 (2012).
18. J. Gao, H. Bai, X. Zhou, G. Yang, C. Xu, Q. Zhang, F. Chen, and Q. Fu, *Nanotechnology*, **25**, 025702 (2014).
19. J. Bian, X. W. Wei, H. L. Lin, S. J. Gong, H. Zhang, and Z. P. Guan, *Polym. Degrad. Stab.*, **96**, 1833 (2011).
20. Y. Lee, D. Kim, J. Seo, H. Han, and S. B. Khan, *Polym. Int*., **62**, 1386 (2013).
21. J. Bian, X. W. Wei, H. L. Lin, L. Wang, and Z. P. Guan, *J. Appl. Polym. Sci*., **124**, 3547 (2012).
22. Y. F. Zhao, M. Xiao, S. J. Wang, X. C. Ge, and Y. Z. Meng, *Compos. Sci. Technol*., **67**, 2528 (2007).
23. H. Kwon, D. Kim, and J. Seo, *Polym. Compos*., **37**, 1744 (2016).
24. J. Yang, L. Bai, G. Feng, X. Yang, M. Lv, C. Zhang, H. Hu, and X. Wang, *Ind. Eng. Chem. Res*., **52**, 16745 (2013).
25. H. Kim, A. A. Abdala, and C. W. Macosko, *Macromolecules*, **43**, 6515 (2010).
26. D. D. L. Chung, *J. Mater. Sci*., **22**, 4190 (1987).
27. T. Wei, Z. Fan, G. Luo, C. Zheng, and D. Xie, *Carbon*, **47**, 337 (2008).
28. J. Bian, H. L. Lin, F. X. He, L. Wang, X. W. Wei, I. T. Chang, and E. Sancaktar, *Eur. Polym. J*., **49**, 1406 (2013).
29. J. Liang, Y. Huang, L. Zhang, Y. Wang, Y. Ma, T. Guo, and Y. Chen, *Adv. Funct. Mater.*, **19**, 2297 (2009).
30. A. M. Pinto, J. Cabral, D. A. P. Tanaka, A. M. Mendes, and F. D. Magalhaes, *Polym. Int*., **62**, 33 (2013).
31. H. J. Kim and S. W. Kim, *J. Appl. Polym. Sci*., **133**, 42973 (2016).
32. J. W. Rhim, *Food Sci. Biotechnol*., **16**, 691 (2007).